

MRI EVALUATION OF KNEE CARTILAGE

Marcelo Bordalo Rodrigues¹, Gilberto Luís Camanho²

ABSTRACT

Through the ability of magnetic resonance imaging (MRI) to characterize soft tissue noninvasively, it has become an excellent method for evaluating cartilage. The development of new and faster methods allowed increased resolution and contrast in evaluating chondral structure, with greater diagnostic accuracy. In addition, physiological techniques for cartilage assessment that can detect early changes before the appearance of cracks and erosion have been developed. In this updating article, the various techniques for chondral assessment using knee MRI will be discussed and demonstrated.

Keywords – Knee injuries; Magnetic resonance imaging; Joint cartilage; Knee joint

INTRODUCTION

Hyaline cartilage is a type of fine connective tissue composed of a complex mesh of collagenous fibers, water and proteoglycans⁽¹⁾. Chondral lesions generally progress slowly and the clinical manifestations occur late in the process.

Simple radiography allows indirect evaluation of the cartilage and forms a good option for assessing degenerative disease, in view of the present therapeutic choices. Direct examination of the hyaline cartilage through magnetic resonance imaging (MRI) is indicated particularly in early cases of osteoarthritis with little or no alteration on simple radiography.

As imaging methods have developed, it has become possible to evaluate cartilage impairment at increasingly early stages and ever more accurately. This evolution in imaging methods has advanced alongside the development of new drugs for treating chondral degeneration. However, imaging findings need to be assessed cautiously and always in conjunction with the patient's symptoms, with the aim of avoiding unnecessary treatments.

Magnetic resonance

MRI enables direct evaluation of the hyaline cartilage and reflects its biochemical and histological complexity.

It is considered to be the best noninvasive method for assessing the joint cartilage because of its high soft-tissue contrast⁽²⁻⁵⁾. Through conventional techniques, it supplies information on chondral thickness, morphological abnormalities of the chondral surface, changes in signal within cartilage substances and abnormalities of the subchondral bone. Through more recent techniques, MRI supplies information on the biochemical and physiological characteristics of the hyaline cartilage. Thus, MRI has become increasingly sensitive with regard to detecting early chondral lesions.

Conventional techniques

Studying the hyaline cartilage depends on obtaining images with high spatial resolution⁽⁶⁾. MRI equipment has developed greatly over recent years, with improvements in gradients and radiofrequency coils. With the present-day equipment, 1.5-Tesla magnets provide cartilage images of excellent spatial resolution. The MRI sequences used for studying joint cartilage are of T1-weighted, proton-density and T2-weighted types. T1-weighted sequences are not useful for evaluating cartilage but, rather, for evaluating the subchondral bone. T2-weighted sequences evaluate the subchondral bone and the interface between the cartilage and the synovial

1 – Radiologist and Director of the Radiology Service, Institute of Orthopedics and Traumatology (IOT), Hospital das Clínicas, University of São Paulo School of Medicine, SP, Brazil.

2 – Titular Professor of the Department of Orthopedics and Traumatology, University of São Paulo School of Medicine, SP, Brazil

Work performed at the Institute of Orthopedics and Traumatology, Hospital das Clínicas, University of São Paulo School of Medicine.

Correspondence: Rua Dr. Ovídio Pires de Campos 333, Têrreo, 05403-010 São Paulo, SP. E-mail: mbordalo@uol.com.br

We declare that there is no conflict of interests in this article

fluid, with less distinction between changes in the intrinsic signal of the hyaline cartilage. For direct viewing of the hyaline cartilage, the proton density-weighted sequence provides greater contrast in its structure and also evaluates the cartilage-synovial fluid interface and the subchondral bone. Currently, the proton density-weighted sequence is considered to present the greatest accuracy for detecting chondral lesions⁽⁷⁻⁹⁾. Volumetric sequences using gradient echoes (echo gradient and SPGR) supply images with high spatial resolution and are indicated for quantification of the chondral morphology. Their disadvantages include lower contrast between the cartilage and the synovial fluid and the long acquisition time required⁽¹⁰⁻¹³⁾. However, several volumetric sequences based on gradient echoes are under development, with the aim of augmenting the contrast of the cartilage-synovial fluid interface and shortening the acquisition time^(14,15) (Figure 1, A and B).

Over the last two years, the use of high field strength magnets has increased in clinical practice, especially 3-Tesla magnets⁽¹⁶⁾. These magnets make it possible to acquire morphological images at higher spatial resolution, which would be impossible to achieve over a reasonable acquisition time using 1.5-Tesla apparatus (Figure 2). Nevertheless, there is still a lack of studies in the literature that might demonstrate whether the use of 3-Tesla magnets provides any increase in accuracy for detecting chondral lesions, in relation to 1.5-Tesla magnets.

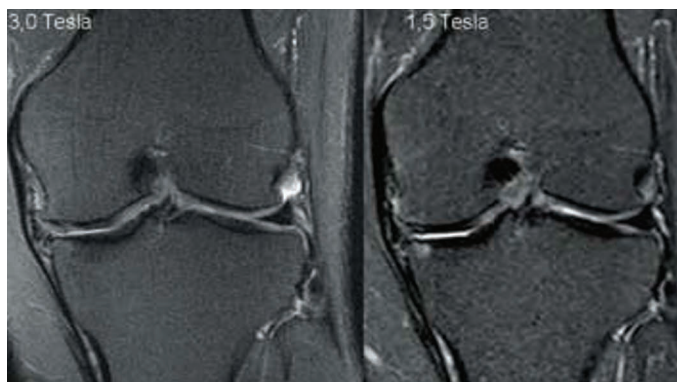


Figure 2 – Comparison between 3.0 and 1.5 Tesla. Coronal T2-weighted MRI with fat saturation on the same patient performed on 3.0 and 1.5-Tesla apparatus. There is greater spatial resolution in the image from the 3.0-Tesla apparatus, with greater definition of the chondral thickness of the medial and lateral compartments. There is also greater definition of the outlines of the marginal and meniscal osteophytes.

Normal cartilage

By using MRI techniques with high spatial resolution and good soft-tissue contrast, a three-layer pattern can be observed in the hyaline cartilage: 1) surface layer with low-intensity signal; 2) intermediate layer with high-intensity signal; and 3) deep layer with low-intensity signal and a “palisade” transition into the intermediate zone. This three-layer appearance is more evident in cartilage of greater thickness, such as the patellar and femoral trochlear cartilage (Figure 3).

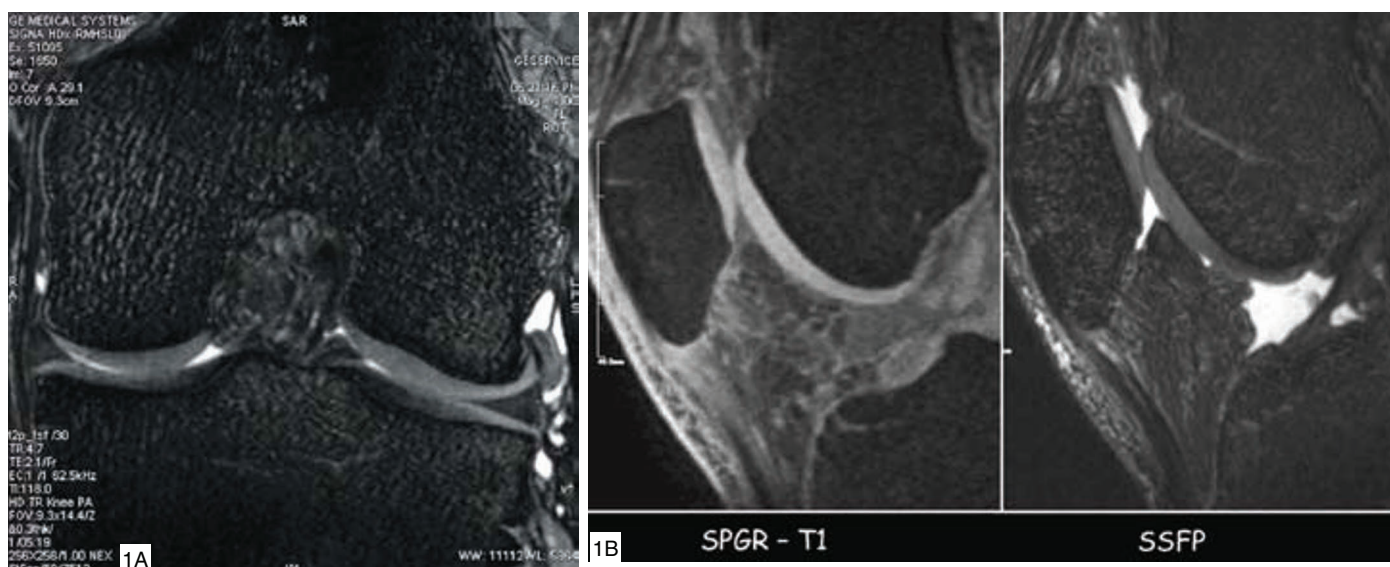


Figure 1 – Gradient echo sequences: (A) SSFP (Steady State Free Precession) sequence in the coronal plan. Note the high definition of the chondral surface of the femoral condyles and tibial plateaus. (B) Comparison between the gradient echo sequences from the same patient: the SSFP sequence presents greater surface definition and greater contrast with the synovial fluid, in relation to the SPGR (Spoiled Gradient Recalled) sequence.



Figure 3 – Three-layered appearance of the hyaline cartilage. Axial T2-weighted MRI of the patella with fat saturation, demonstrating the three-layered appearance of the hyaline cartilage. The deepest layer presents low-intensity signal (arrow); the intermediate layer, high-intensity signal (black arrowhead); and the surface layer, low-intensity signal (white arrowhead).

Chondral lesions

The accuracy of MRI for detecting chondral lesions depends on the MRI technique used and, especially, on the size of the lesion. In cases of superficial fibrillation, conventional MRI with protocols optimized for cartilage evaluation presents low diagnostic accuracy. The accuracy is greater in deeper lesions, particularly in those that present more than 50% loss of chondral substance, with values in the literature ranging from 73 to 96%^(17,18).

Chondral lesions are diagnosed through signal, thickness and morphological abnormalities of the hyaline cartilage. The most specific MRI signal for chondral le-

sions is the presence of areas of greater signal in proton density and T2-weighted sequences and on the echo gradient. However, this signal does not have the sensitivity to determine lesion presence. A study demonstrated that 70% of chondral lesions presented a high signal in relation to normal cartilage on the proton density sequence, while 20% presented a signal similar to that of normal cartilage (i.e. lesions were not seen on MRI) and 10% presented a low signal in relation to normal cartilage. It was also demonstrated that high-signal lesions were more extensive than were lesions with the same signal or low signal⁽¹⁹⁾.

Chondral tapering, loss of definition of the cartilage outline and surface irregularities are other signals that help in the evaluation.

It has been demonstrated that the most frequent locations for chondral lesions are the medial femoral condyle (on its most internal aspect) and the lateral tibial plateau (on its most posterior portion)⁽²⁰⁾ (Figure 4, A and B).

To classify chondral lesions using MRI, a system based on arthroscopic classifications is used⁽²¹⁻²³⁾. Grade I lesions are shown as abnormalities of focal signals within cartilage substances, corresponding to softening of the cartilage seen on arthroscopy. Grade II lesions are shown as abnormalities of the surface signal, indicating fibrillation or erosion of less than 50% of the chondral thickness. In Grade III lesions, there is loss of more than 50% of the chondral substance and there may be small areas in which the bone surface is reached. Grade IV lesions indicate extensive full-thickness chondral defects with bone marrow edema (Figure 5, A to D).

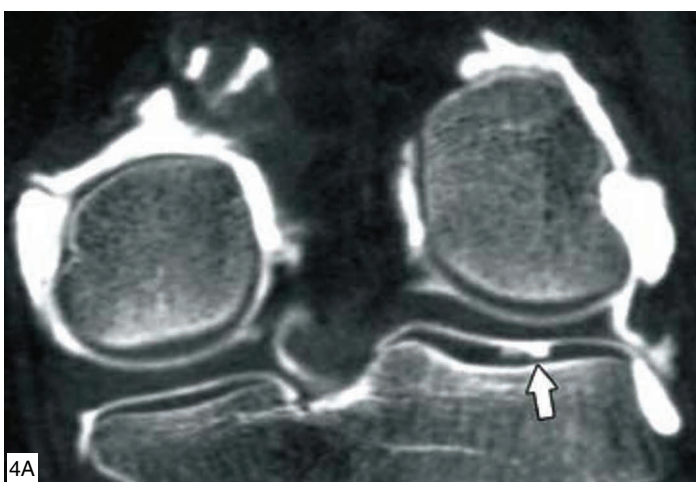


Figure 4 – Commonest locations for chondral lesions of the knee, seen on arthro-CT with coronal reformatting. (A) Chondral lesion in the posterior portion of the lateral tibial plateau (arrow). (B) Chondral lesion on the most internal aspect of the medial femoral condyle (arrowhead).

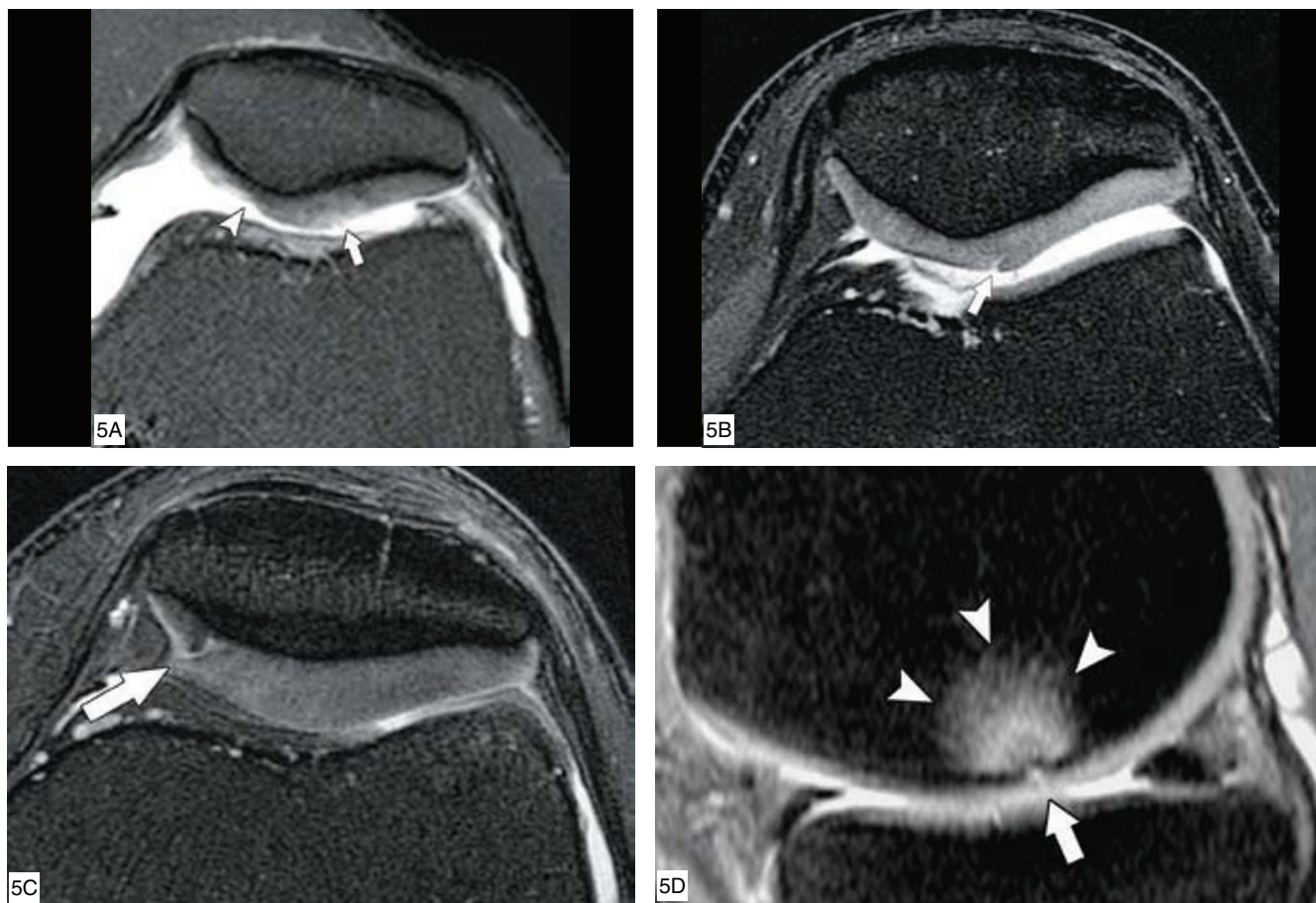


Figure 5 – Classification of chondral lesions of the knee. Axial MRI (A to C) and sagittal MRI (D) with T2 weighting and fat saturation. (A) Slight elevation of the surface signal from the hyaline cartilage of the lateral facet of the patella (arrow), indicating grade I chondropathy. There is also deep chondral erosion (grade III) on the medial facet (arrowhead). (B) Chondral fissure affecting less than 50% of the total thickness of the lateral facet of the patella, indicating grade II chondropathy (arrow). (C) Chondral fissure affecting more than 50% of the total thickness of the medial facet of the patella, indicating grade III chondropathy (arrow). (D) Deep chondral fissure in the lateral femoral condyle (arrow), reaching the subchondral bone and presenting edema in the adjacent bone marrow (arrowheads), characterizing grade IV chondropathy.

Alterations to the subchondral bone

Loss of joint cartilage integrity may cause abnormalities in the underlying bone, such as cysts (geodes), sclerosis and osteophytosis, which can be detected by means of MRI (Figure 6, A to C). Another frequently associated finding is elevation of the subchondral bone signal, which is known as bone edema but in reality is the expression of a variety of histological abnormalities such as necrosis, fibrosis and trabecular microfractures⁽²⁴⁾. It has been demonstrated that subchondral cysts develop in preexisting areas of “subchondral bone edema”⁽²⁵⁾.

Synovial abnormalities

Chronic chondral lesions with detachment of cartilaginous fragments into the joint lead to chronic irritation of the synovium and may cause synovitis. In some cases, the synovial response is very extensive and may take on

a pseudotumoral appearance on imaging examinations (Figure 7, A to C). It is also common for there to be free bodies in the joints, especially in the suprapatellar recesses, posteriorly to the femorotibial and popliteal joints.

Secondary joint alterations

Arthrosis may also lead to certain secondary joint alterations. Among these are degenerative lesions of the medial meniscus and osteonecrosis with joint collapse (Figures 8 and 9, A and B).

Physiological assessment of the hyaline cartilage by means of MRI

The hyaline cartilage consists of water (70% of the weight), type II collagen and proteoglycans. Through techniques for MRI acquisition and evaluation, the biochemical composition of the hyaline cartilage can be

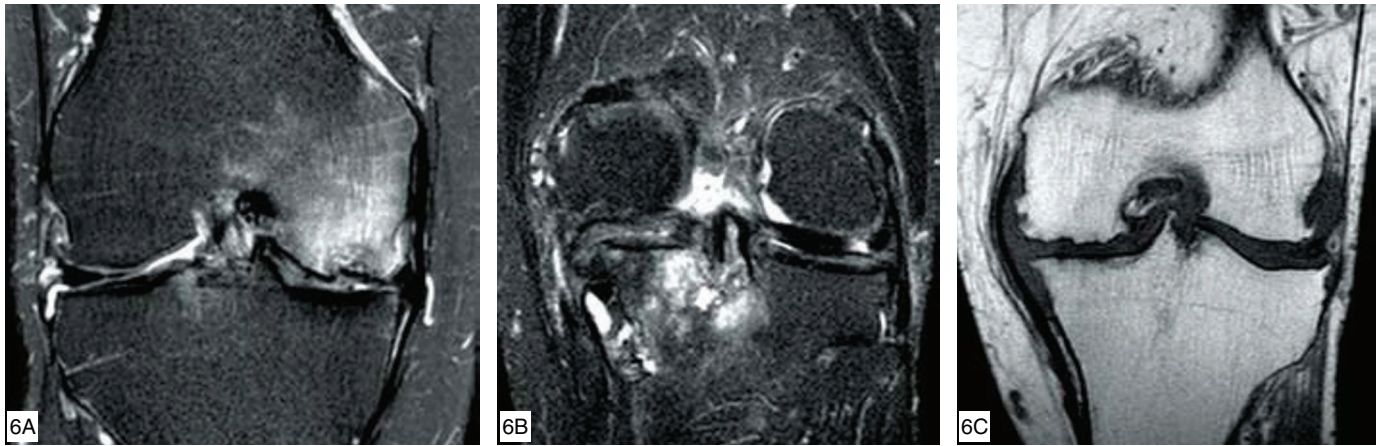


Figure 6 – Subchondral abnormalities seen on MRI. Coronal fast-saturated MRI on the knee, with T2 weighting (A and B) and T1 weighting (C). (A) Reduction of the chondral thickness on the medial femoral condyle, with bone marrow edema and a small fracture in the subchondral cortical bone. (B) Femorotibial degenerative arthropathy with subchondral cysts and bone marrow edema on the medial tibial plateau. (C) Medial and lateral femorotibial degenerative arthropathy with marginal osteophytes.

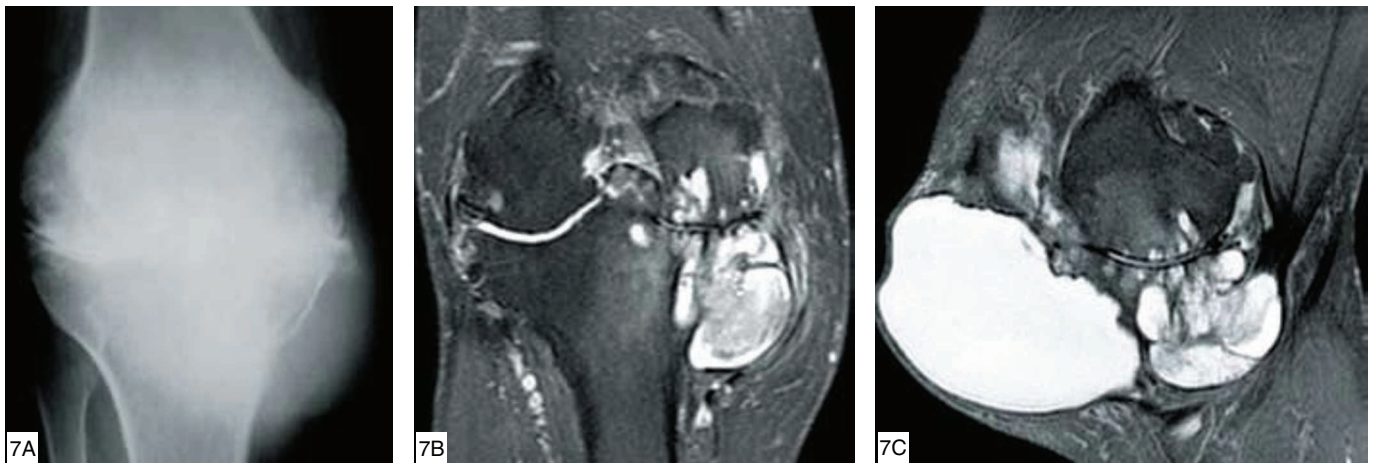


Figure 7 – Synovial metaplasia secondary to severe arthropathy with a pseudotumoral appearance. (A) AP radiography of the knee, demonstrating severe grade V Ahlbäck arthropathy with increased soft tissue at the medial tibial plateau. Coronal MRI (B) and sagittal MRI (C) with T2 weighting and fat saturation, showing large subchondral cysts on the tibial plateau and femoral condyle, and a large anterior synovial cyst secondary to metaplasia.

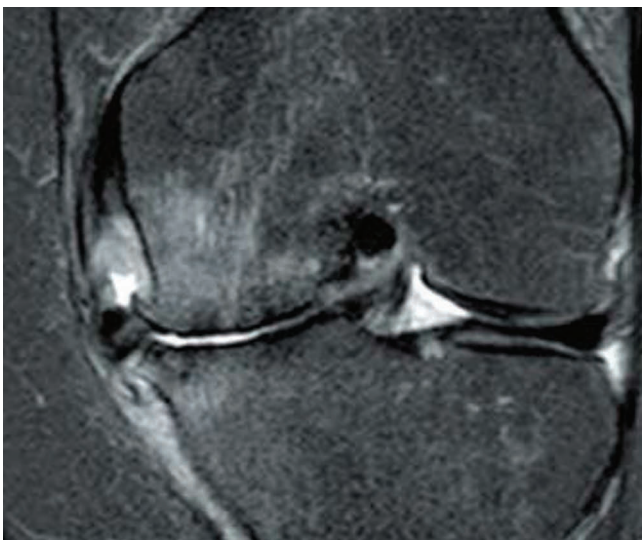


Figure 8 – Degenerative meniscal lesion secondary to severe arthropathy. Medial femorotibial degenerative arthropathy associated with extrusion of the medial meniscal body, which presents signal elevation and synovitis surrounding it, thus indicating a degenerative lesion.

assessed. These techniques are still at the research stage, but they are promising in relation to their clinical application in the near future, especially in relation to early detection of chondral lesions before their manifestation as macroscopic anatomical lesions. In the following, some of these techniques will be described briefly:

– T2 mapping: This assesses the water content and ultrastructure of the tissue collagen. The T2 relaxation time measurement demonstrates areas of greater or smaller water content, depending on the chondral lesion⁽²⁶⁻²⁸⁾. This measurement is represented by a map on a scale of colors. Longer T2 relaxation time in focal areas of cartilage is associated with damage to the chondral matrix and, especially, loss of collagen integrity (Figure 10, A and B).

– T1-rho mapping: This is a promising technique that is very sensitive for evaluating early depletion of proteoglycans^(29,30).

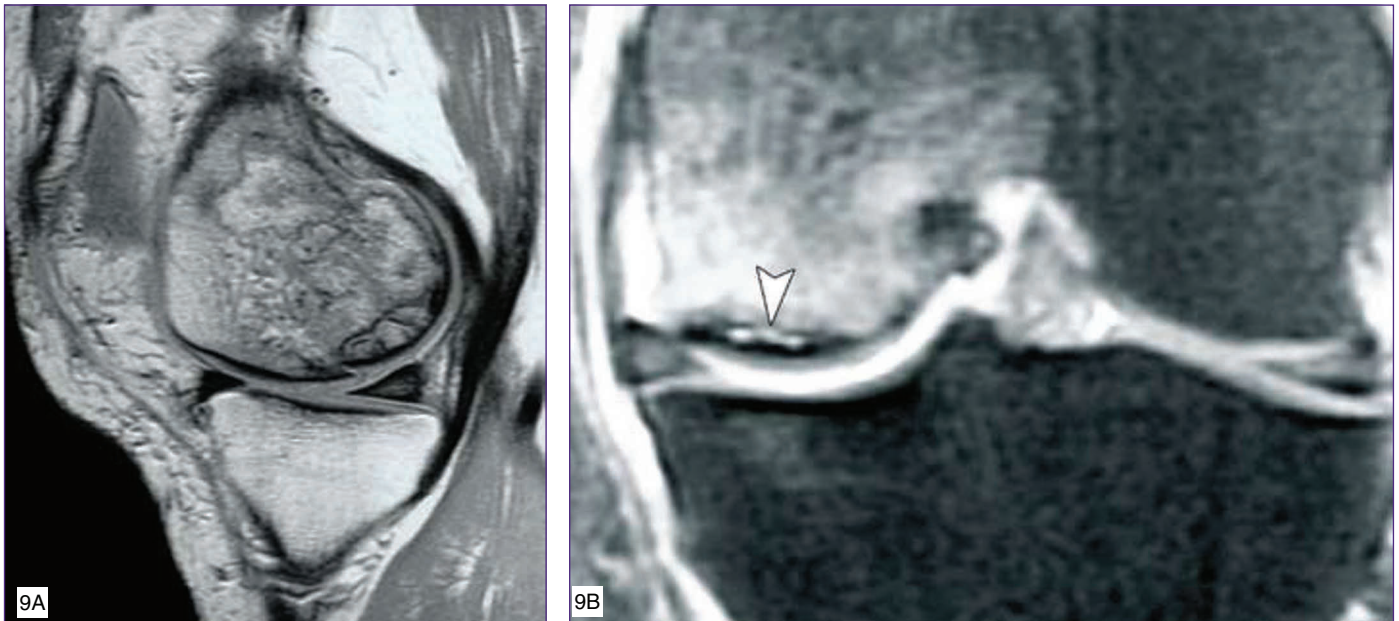


Figure 9 – Osteonecrosis of the femoral condyle. (A) Sagittal T1-weighted MRI showing geographical lesion on the medial femoral condyle, with an adjacent subchondral bone lamina fracture. (B) Coronal T2-weighted MRI with fat saturation showing severe degenerative arthropathy with bone necrosis on the medial femoral condyle, associated with a fracture of the adjacent subchondral bone lamina (arrowhead).

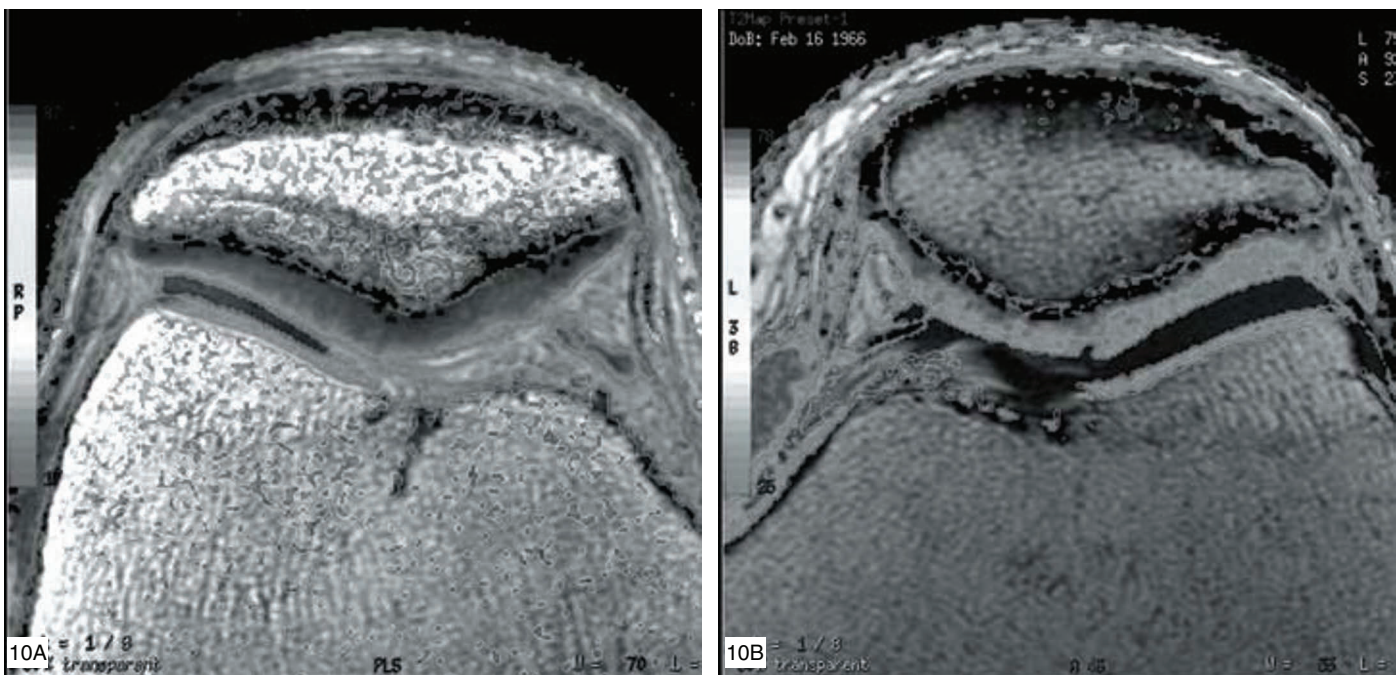


Figure 10 – Functional image of the cartilage: T2 mapping. (A) Axial image of the patella with T2 mapping represented by the scale of colors, demonstrating cartilage with homogenous normal T2 times (around 20 msec), thus indicating normal cartilage. (B) Note an increase in the T2 times (around 40-50 msec), demonstrated by the color map (arrows) and distributed heterogeneously, and more markedly on the lateral facet, thus indicating structural damage to the chondral matrix. A small fissure on the medial facet is also seen (arrowhead).

– d-GMERIC (delayed gadolinium-enhanced MRI of cartilage): Proteoglycan consists of glycosaminoglycan chains with abundant positive charges. The paramagnetic contrast most used is gadolinium (Gd-DTPA), and this also presents negative charges. After intravenous injection,

the paramagnetic contrast penetrates the cartilage and is distributed to areas with low glycosaminoglycan concentration^(28,31-33). Through a T1 map, the Gd-DTPA concentration can be quantified and, consequently, the glycosaminoglycan content.

REFERENCES

1. Buckwalter JA, Mankin HJ. Articular cartilage: tissue design and chondrocyte-matrix interactions. *Instr Course Lect*. 1998;47:477-86.
2. Recht MP, Resnick D. Magnetic resonance imaging of articular cartilage: an overview. *Top Magn Reson Imaging*. 1998;9(6):328-36.
3. Recht M, Bobic V, Burstein D, Disler D, Gold G, Gray M, et al. Magnetic resonance imaging of articular cartilage. *Clin Orthop Relat Res*. 2001;(391 Suppl):S379-96.
4. Hodler J, Resnick D. Current status of imaging of articular cartilage. *Skeletal Radiol*. 1996; 25(8):703-9.
5. Disler DG, McCauley TR. Clinical magnetic resonance imaging of articular cartilage. *Top Magn Reson Imaging*. 1998;9(6):360-76.
6. Rubenstein JD, Li JG, Majumdar S, Henkelman RM. Image resolution and signal-to-noise ratio requirements for MR imaging of degenerative cartilage. *AJR Am J Roentgenol*. 1997;169(4):1089-96.
7. Schaefer FK, Kurz B, Schaefer PJ, Fuerst M, Hedderich J, Graessner J, et al. Accuracy and precision in the detection of articular cartilage lesions using magnetic resonance imaging at 1.5 Tesla in an in vitro study with orthopedic and histopathologic correlation. *Acta Radiol*. 2007;48(10):1131-7.
8. Mohr A. The value of water-excitation 3D FLASH and fat-saturated PDw TSE MR imaging for detecting and grading articular cartilage lesions of the knee. *Skeletal Radiol*. 2003;32(7):396-402.
9. Pötter HG, Linklater JM, Allen AA, Hannafin JA, Haas SB. Magnetic resonance imaging of articular cartilage in the knee. An evaluation with use of fast-spin-echo imaging. *J Bone Joint Surg Am*. 1998;80(9):1276-84.
10. Ciuttini F, Forbes A, Asbeutah A, Morris K, Stuckey S. Comparison and reproducibility of fast and conventional spoiled gradient-echo magnetic resonance sequences in the determination of knee cartilage volume. *J Orthop Res*. 2000;18(4):580-4.
11. Eckstein F, Schnier M, Haubner M, Priebsch J, Glaser C, Englmeier KH, et al. Accuracy of cartilage volume and thickness measurements with magnetic resonance imaging. *Clin Orthop Relat Res*. 1998;(352):137-48.
12. Eckstein F, Winzheimer M, Westhoff J, Schnier M, Haubner M, Englmeier KH, et al. Quantitative relationships of normal cartilage volumes of the human knee joint—assessment by magnetic resonance imaging. *Anat Embryol (Berl)*. 1998;197(5):383-90.
13. Eckstein F, Westhoff J, Sittek H, Maag KP, Haubner M, Faber S, et al. In vivo reproducibility of three-dimensional cartilage volume and thickness measurements with MR imaging. *AJR Am J Roentgenol*. 1998;170(3):593-7.
14. Yoshioka H, Stevens K, Hargreaves BA, Steines D, Genovese M, Dillingham MF, et al. Magnetic resonance imaging of articular cartilage of the knee: comparison between fat-suppressed three-dimensional SPGR imaging, fat-suppressed FSE imaging, and fat-suppressed three-dimensional DEFT imaging, and correlation with arthroscopy. *J Magn Reson Imaging*. 2004;20(5):857-64.
15. Kornaat PR, Reeder SB, Koo S, Brittain JH, Yu H, Andriacchi TP, et al. MR imaging of articular cartilage at 1.5T and 3.0T: comparison of SPGR and SSFP sequences. *Osteoarthritis Cartilage*. 2005;13(4):338-44.
16. Gold GE, Hargreaves BA, Stevens KJ, Beaulieu CF. Advanced magnetic resonance imaging of articular cartilage. *Orthop Clin North Am*. 2006;37(3):331-47.
17. Azer NM, Winalski CS, Minas T. MR imaging for surgical planning and postoperative assessment in early osteoarthritis. *Radiol Clin North Am*. 2004;42(1):43-60.
18. Vande Berg BC, Lecouvet FE, Poivache P, Jamart J, Materne R, Lengele B, et al. Assessment of knee cartilage in cadavers with dual-detector spiral CT arthrography and MR imaging. *Radiology*. 2002;222(2):430-6.
19. Vande Berg BC, Lecouvet FE, Maldague B, Malghem J. MR appearance of cartilage defects of the knee: preliminary results of a spiral CT arthrography-guided analysis. *Eur Radiol*. 2004;14(2):208-14.
20. Vande Berg BC, Lecouvet FE, Malghem J. Frequency and topography of lesions of the femoro-tibial cartilage at spiral CT arthrography of the knee: a study in patients with normal knee radiographs and without history of trauma. *Skeletal Radiol*. 2002;31(11):643-9.
21. Bachmann G, Heinrichs C, Jurgensen I, Rominger M, Scheiter A, Rau WS. [Comparison of different MRT techniques in the diagnosis of degenerative cartilage diseases. In vitro study of 50 joint specimens of the knee at T1.5]. *Rofo*. 1997;166(5):429-36.
22. Outerbridge RE. The etiology of chondromalacia patellae. *J Bone Joint Surg Br*. 1961; 43:752-757.
23. Shahriaree H. Chondromalacia. *Contemp Orthop*. 1985;11(1):27-39.
24. Zanetti M, Bruder E, Romero J, Hodler J. Bone marrow edema pattern in osteoarthritic knees: correlation between MR imaging and histologic findings. *Radiology*. 2000;215(3):835-40.
25. Carrino JA, Blum J, Parellada JA, Schweitzer ME, Morrison WB. MRI of bone marrow edema-like signal in the pathogenesis of subchondral cysts. *Osteoarthritis Cartilage*. 2006;14(10):1081-5.
26. Poon CS, Henkelman RM. Practical T2 quantitation for clinical applications. *J Magn Reson Imaging*. 1992;2(5):541-53.
27. Goodwin DW, Zhu H, Dunn JF. In vitro MR imaging of hyaline cartilage: correlation with scanning electron microscopy. *AJR Am J Roentgenol*. 2000;174(2):405-9.
28. Burstein D, Bashir A, Gray ML. MRI techniques in early stages of cartilage disease. *Invest Radiol*. 2000;35(10):622-38.
29. Duvvuri U, Charagundla SR, Kudchodkar SB, Kaufman JH, Kneeland JB, Rizi R, et al. Human knee: in vivo T1(rho)-weighted MR imaging at 1.5 T—preliminary experience. *Radiology*. 2001;220(3):822-6.
30. Regatte RR, Akella SV, Borthakur A, Kneeland JB, Reddy R. In vivo proton MR three-dimensional T1rho mapping of human articular cartilage: initial experience. *Radiology*. 2003;229(1):269-74.
31. Tiderius CJ, Tjornstrand J, Akesson P, Sodersten K, Dahlberg L, Leander P. Delayed gadolinium-enhanced MRI of cartilage (dGEMRIC): intra- and interobserver variability in standardized drawing of regions of interest. *Acta Radiol*. 2004;45(6):628-34.
32. Tiderius CJ, Svensson J, Leander P, Ola T, Dahlberg L. dGEMRIC (delayed gadolinium-enhanced MRI of cartilage) indicates adaptive capacity of human knee cartilage. *Magn Reson Med*. 2004;51(2):286-90.
33. Kim YJ, Jaramillo D, Millis MB, Gray ML, Burstein D. Assessment of early osteoarthritis in hip dysplasia with delayed gadolinium-enhanced magnetic resonance imaging of cartilage. *J Bone Joint Surg Am*. 2003;85(10):1987-92.